CHAPTER 5

DIELECTRIC PROPERTIES AND MORPHOTROPIC PHASE BOUNDARY IN THE xPb($Zn_{1/3}Nb_{2/3}$)O_3–($1-x$)Pb($Zr_{0.5}Ti_{0.5}$)O_3 PSEUDO-BINARY SYSTEM

Overview – Ceramics in the xPb($Zn_{1/3}Nb_{2/3}$)O_3–$(1-x)$Pb($Zr_{0.5}Ti_{0.5}$)O_3 [xPZN–($1-x$)PZT] solid solution system are expected to display excellent dielectric, piezoelectric, and ferroelectric properties in compositions close to the morphotropic phase boundary (MPB). The dielectric behavior of ceramics with $x = 0.1 - 0.6$ has been characterized in order to identify the MPB compositions in this system. Combined with x-ray diffraction results, ferroelectric hysteresis measurements, and Raman reflectivity analysis, it was consistently shown that an MPB exists around $x = 0.25$ in this binary system. When $x \leq 0.2$, the tetragonal phase dominates at ambient temperatures. In the range of $x \geq 0.3$, the rhombohedral phase dominates. For this rhombohedral phase, electrical measurements reveal profound frequency dispersion in the dielectric response when $x \geq 0.6$, suggesting a transition from normal ferroelectric to relaxor ferroelectric between $0.5 \leq x \leq 0.6$. Excellent piezoelectric properties were found in 0.3PZN–0.7PZT, the composition closest to the MPB with a rhombohedral structure. The results are summarized in a PZN–PZT binary phase diagram.

5.1 Introduction

Piezoelectric materials are widely used for various devices, including multilayer capacitors, sensors, and actuators. By the 1950's, the ferroelectric solid solution $Pb(Zr_{1-x}Ti_x)O_3$ (PZT) was found to host exceptionally high dielectric and piezoelectric properties for compositions close to the morphotropic phase boundary (MPB).[2] This MPB is located around $PbZrO_3$:$PbTiO_3$ ~ 0.52:0.48 and separates a Ti-rich tetragonal phase from a Zr-rich rhombohedral phase.[2] Most commercial PZT ceramics are thus designed in the vicinity of the MPB with various dopings in order to achieve optimum properties.

$Pb(Zn_{1/3}Nb_{2/3})O_3$ (PZN) is an important relaxor ferroelectric material with the rhombohedral structure at room temperature. A diffuse phase transition from the paraelectric state to a ferroelectric polar state occurs at 140°C.[25] Extensive research has been carried out on PZN single crystals because of their excellent dielectric, electrostrictive, and optical properties.[21] Although single crystals of PZN can routinely be grown by the flux method,[25] it is known that perovskite PZN ceramics cannot be synthesized by the conventional mixed-oxide method without doping.[18,27,28] Attempts to synthesize perovskite PZN ceramics invariably results in the formation of a pyrochlore phase with accompanying degradation of the dielectric and piezoelectric properties. Various chemical additives, such as $Ba(Zn_{1/3}Nb_{2/3})O_3$, $BaTiO_3$, and $SrTiO_3$ have thus been explored in an attempt to stabilize the perovskite PZN ceramic.[16] However, a trade-off is made with these additives leading to reduced dielectric constants and piezoelectric coefficients. Therefore, there is significant interest in finding a method to stabilize the perovskite phase in PZN without sacrificing the excellent dielectric and piezoelectric properties.

Recent work has shown that ultra-high piezoelectric properties can be obtained in relaxor-normal ferroelectric solid solutions with compositions close to the MPB, such as the $Pb(Mg_{1/3}Nb_{2/3})O_3$–$PbTiO_3$ system[54] and the $Pb(Zn_{1/3}Nb_{2/3})O_3$–$PbTiO_3$ system.[25] Since both PZT and PZN have the perovskite structure and both are known to have excellent dielectric and piezoelectric properties, one approach to stabilize and optimize PZN ceramics is to alloy PZN with PZT. Fan *et al*[24] have successfully produced phase-pure perovskite of $xPb(Zn_{1/3}Nb_{2/3})O_3$–$(1-x)Pb(Zr_{0.47}Ti_{0.53})O_3$ ceramics in the range of $0.4 \leq x \leq 0.7$ via the conventional mixed-oxide method and observed excellent properties near the MPB composition. In chapter 4 shown that a compared the conventional mixed-oxide method with the columbite method in the preparation of a similar system $xPb(Zn_{1/3}Nb_{2/3})O_3$–$(1-x)Pb(Zr_{0.5}Ti_{0.5})O_3$ [*x*PZN–(*1-x*)PZT] and found that the columbite method leads to better compositional homogeneity and ferroelectric properties. In this chapter will give further information on the dielectric and piezoelectric properties and phase transitions in this *x*PZN–(*1-x*)PZT binary system prepared by both methods, with the purpose of confirming improved properties in ceramics synthesized via the columbite method.

5.2 Experimental procedure

For the conventional method, regent grade oxides of PbO, ZnO, ZrO_2, TiO_2 and Nb_2O_5 were mixed in the required stoichiometric ratios for the general composition *x*PZN–*(1-x)*PZT where *x = 0.1, 0.2, 0.3, 0.4, 0.5* and *0.6*. An additional 2 mol% excess PbO was added to account for PbO volatility. After ball milling for 24 hours and drying at 120°C, the mixture was calcined at temperatures between 750 to

950 ^{o}C for 4 hours using a double crucible configuration.[50] A heating rate of 20^{o}C/min[50] was selected for all of the compositions in this system. For the columbite method, the columbite precursor $ZnNb_2O_6$ was prepared from the reaction between ZnO (99.9%) and Nb_2O_5 (99.9%) at 975^{o}C for 4 hours. The wolframite precursor $ZrTiO_4$ was formed by reacting ZrO_2 (99.9%) with TiO_2 (99.9%) at 1400^{o}C for 4 hours.[51] The precursors $ZnNb_2O_6$, $ZrTiO_4$ were then mixed with PbO (99.9%) according to the stoichiometric ratio for the desired compositions with 2 mol% excess PbO added. The mixtures were then followed the same processing conditions as the conventional method. The calcined powders were cold isostatically pressed into pellets at a pressure of 80 MPa. Five sintering conditions were utilized: 1175°C, 1200°C, 1225°C, 1250°C, and 1275°C all with a dwell time of 2 hours. To inhibit PbO volatilization from the pellets, a PbO atmosphere was maintained with a bed of $PbZrO_3$ powder placed in the vicinity of the pellets. The calcined powder and sintered pellets were checked for perovskite phase formation by x-ray diffraction (XRD).

Thin slices cut from sintered pellets were prepared with sputtered gold electrodes for electrical characterization. The relative permittivity (ε_r) and dissipation factor ($tan\ \delta$) were measured with an LCR meter (HP-4284A, Hewlett-Packard Inc.) at frequencies of 0.1, 1, 10, and 100 kHz in conjunction with an environmental chamber with a temperature range of 25 – 450^{o}C. A heating rate of 3^{o}C/minute was used during measurements. The piezoelectric coefficient (d_{33}) was measured with a d_{33} meter (Model 8000 d_{33} Tester) on poled slices. The electromechanical coupling factor (k_p) was calculated according to the resonance and anti-resonance frequencies obtained with an impedance analyzer (Model 4194A, HP).

Raman scattering was measured on polished specimens using a Renishaw in Via Reflex Raman spectrometer with a 488 nm radiation source. The grain size was evaluated by scanning electron microscopy (SEM) (JSM5410, JEOL) and the ferroelectric domain morphology was examined by transmission electron microscopy (TEM) (CM30, Phillips).

5.3 Results and discussion

5.3.1 Perovskite phase formation and microstructure

Powder XRD was extensively used to monitor the phase development at each step during ceramic preparation to ensure the phase purity. Phase-pure precursors $ZnNb_2O_6$ and $ZrTiO_4$ were obtained using the calcination conditions described previously. The calcined powders for the perovskite solid solutions were also examined by XRD and the results are exemplified by the powders of *0.5*PZN–*0.5*PZT, as shown in Fig. 5.1. Similar trends were apparent for both the conventional method and the columbite method: higher calcination temperatures led to higher perovskite phase purity. At 900°C, the pyrochlore phase disappeared below the resolution limits of XRD. The perovskite phase development at different calcination temperatures was estimated from the XRD data with the commonly used formula mentioned as equation (3.1)

The calculation for the data shown in Fig. 5.1 for the *0.5*PZN–*0.5*PZT powder is plotted in Fig. 5.2, where the peak intensity ratio illustrates the evolution of phase-pure perovskite. The increase in the phase purity with increasing calcination temperature for both methods is evident. It is noted in Fig. 5.2 that the conventional

method showed a higher amount of the perovskite phase than the columbite method below 900°C. Presumably the difference is due to the different reaction paths between the two methods. After sintering of the powders calcined at 900°C, the perovskite phase was preserved as evidenced by XRD with one exception. At the highest PZN concentration of $x = 0.6$, a small amount of pyrochlore phase was detected though the sample remained approximately 98.5% perovskite. The sintered pellets appeared to be dense and the grain size was in the range of 1~5 μm, as shown in Fig. 5.3. The comparison between Fig. 5.3(a) and 5.3(b) indicates that the conventional method produces ceramics with slightly coarser grains.

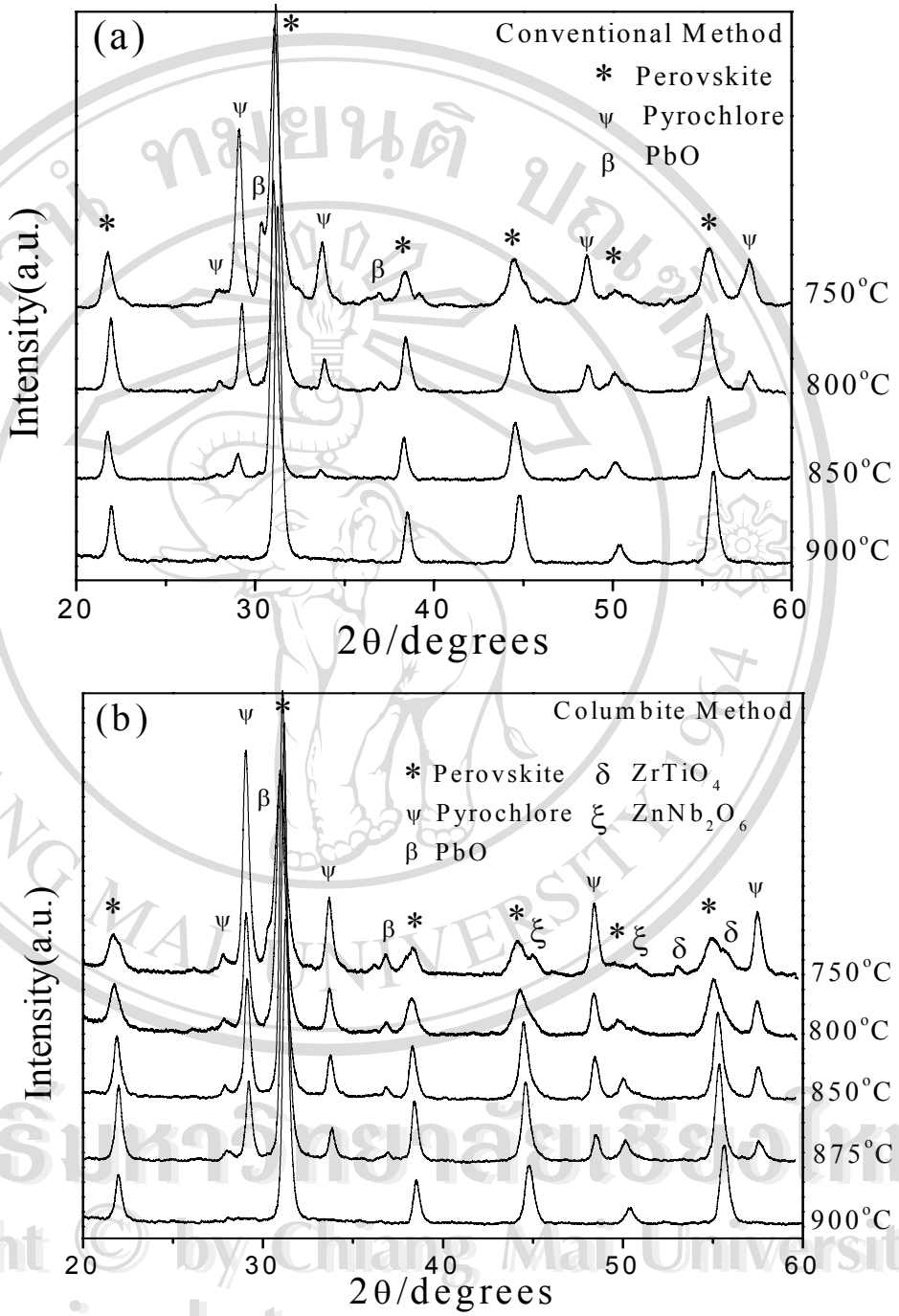

Figure 5.1 XRD spectra of *0.5*PZN–*0.5*PZT powder calcined at various temperatures for 4 hours. (a) the conventional mixed-oxide method; and (b) the columbite method.

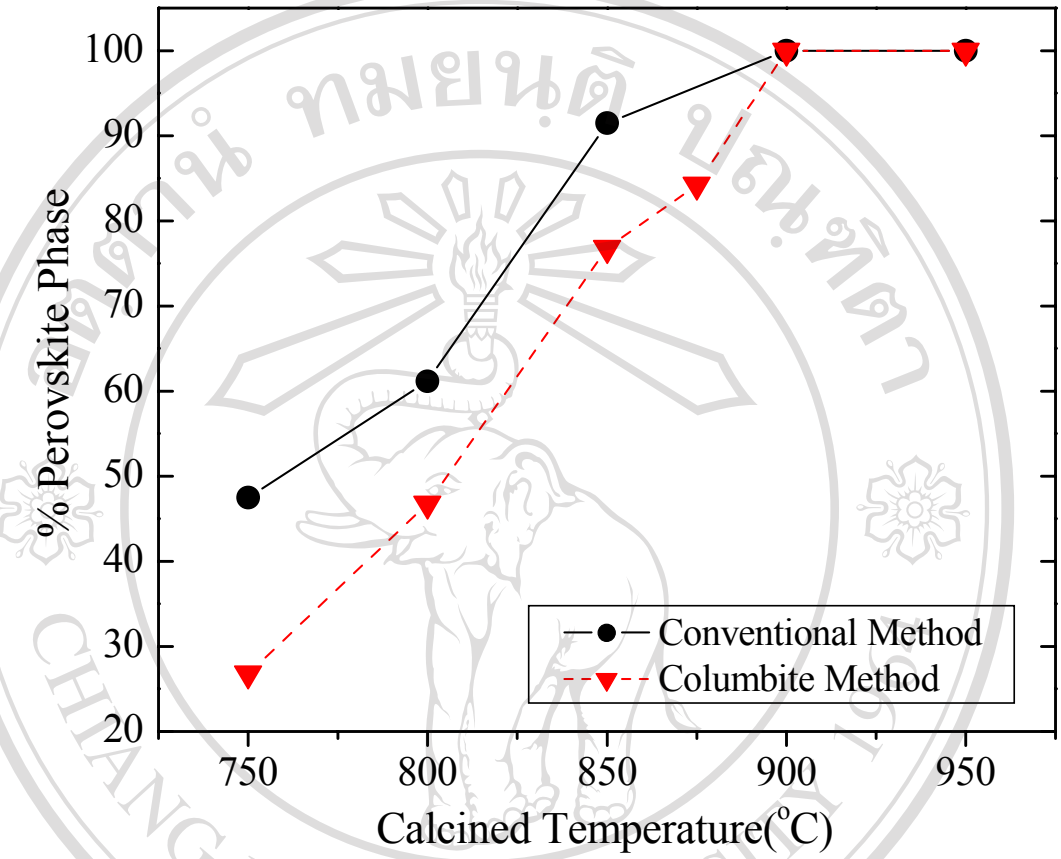

Figure 5.2 Perovskite phase content in *0.5*PZN–*0.5*PZT powders calcined at different temperatures.

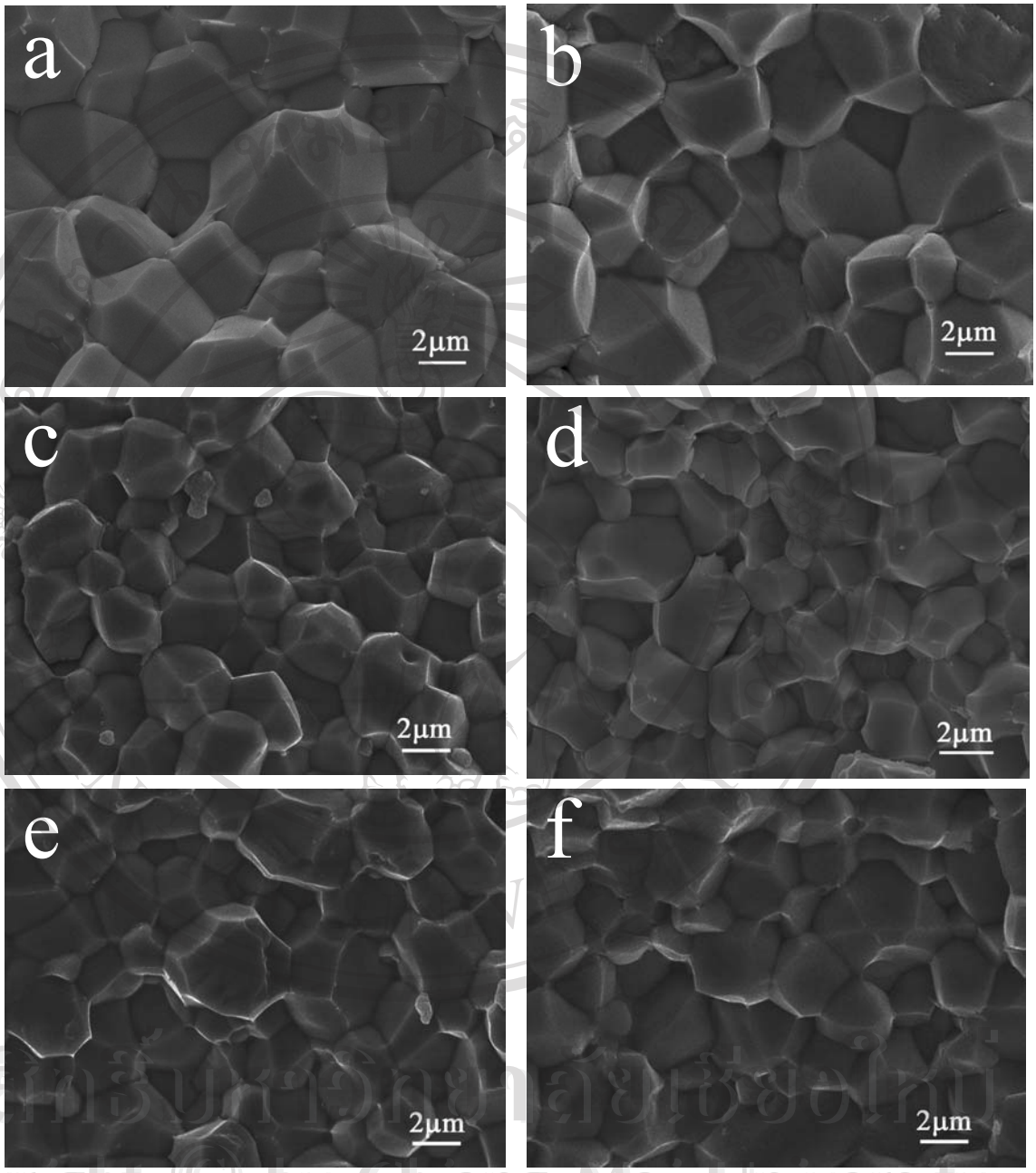

Figure 5.3 SEM examination of the grain morphology in *x*PZN–(*1-x*)PZT ; x = *0.1-0.5* ceramics sintered at optimum sintering condition: (a), (c) and (e) prepared by conventional method; (b), (d) and (f) prepared by columbite method.

5.3.2 Dielectric behavior

The relative permittivity of *x*PZN–(*1-x*)PZT ceramics was measured as a function of temperature up to 450°C at different frequencies. The results are presented in Fig. 5.4 for ceramics prepared by the two methods. It is interesting to note that all compositions show a dispersive dielectric behavior with respect to frequency. However, the frequency dispersion in the PZN–PZT binary system is not as strong as that in the pure relaxor PZN. For all compositions, Table 5.1 lists the temperature at which the permittivity is maximum (T_{max}), and the relative permittivity both at room temperature and at T_{max}. These results show that the permittivity of ceramics prepared via the columbite method was significantly higher than that of ceramics synthesized by the conventional method. It is also evident from Fig. 5.4 and Table 5.1 that *0.2*PZN–*0.8*PZT and *0.5*PZN–*0.5*PZT show the highest peak values of the relative permittivity. For the *0.2*PZN–*0.8*PZT composition, the peak value reads 25,800 for the columbite method and 25,000 for the conventional method. For the *0.5*PZN–*0.5*PZT composition, the peak relative permittivity is 21,200 for the columbite method and 20,800 for the conventional method. The ε_r versus T curves shown in Fig. 5.4 is also indicative of thermally induced phase transitions. These transitions are prominent in the compositions $x = 0.3$, *0.5* and *0.6* as depicted separately in Fig. 5.4(a, b and c).

At the composition $x = 0.3$ two peaks were revealed at temperatures 283.6°C and 298.8°C in the ceramic prepared by the columbite method (Fig. 5.4a). However, this was not observed in ceramics of the same composition prepared via the conventional method. In this case, there was only one peak present at 309°C. The columbite method is anticipated producing ceramics with better compositional

homogeneity than the conventional mixed oxide method. In addition the grain size of ceramics prepared by columbite method is slightly smaller than conventional method. As the grain size decreases the domains become smaller, with the domain width being roughly proportional decreases as the square root of the grain size, and so the smaller the grain the larger is the unrelieved stress. It can be shown using Devonshire's phenomenological theory that an increase in stress is accompanied by an increase in permittivity.[13] For the composition $x = 0.5$, the ε_r versus T curves revealed the occurrence of transitions between normal ferroelectric and relaxor ferroelectric behaviors, as indicated in Fig. 5.4(b). These transitions were observed in ceramics prepared by both methods. In Fig. 5.4(b) which shows the dielectric behavior of the ceramic prepared via the columbite method, a strong frequency dispersion in the permittivity was evident at temperatures $T > 242^oC$ and $T < 235°C$. In the narrow temperature range of $235°C < T < 242^oC$, the permittivity increased precipitously. This temperature range is bounded by $T_{start\ NR}$ and $T_{finish\ NR}$*, as denoted in Fig. 5.4(b). Similar transitions have been observed by other researchers in other solid solution systems.[55] The $x = 0.6$ composition showed a broadening of the permittivity maxima and T_m increased with increasing measurement frequency (Fig. 5.4(c)). This indicates that this composition shows a diffuse phase transition with a strong frequency dispersion which is characteristic of relaxor ferroelectricity.

*The subscript NR stands for the normal ferroelectric↔relaxor ferroelectric transition.

Table 5.1 Comparison of the dielectric properties of *x*PZN–(*1-x*)PZT ceramics prepared by the conventional mixed-oxide and columbite methods.

x	T_{max}(°C)		ε_r at 25°C		ε_r at T_{max}	
	Conventional	Columbite	Conventional	Columbite	Conventional	Columbite
x = 0.1	359	351	810	1,590	13,300	21,200
x = 0.2	329	324	1,230	1,550	25,000	25,800
x = 0.3	309	299	980	1,580	14,300	15,700
x = 0.4	281	273	1,230	1,440	17,000	20,800
x = 0.5	250	242	1,220	1,430	20,800	21,200
x = 0.6	240	231	1,230	1,440	11,400	13,200

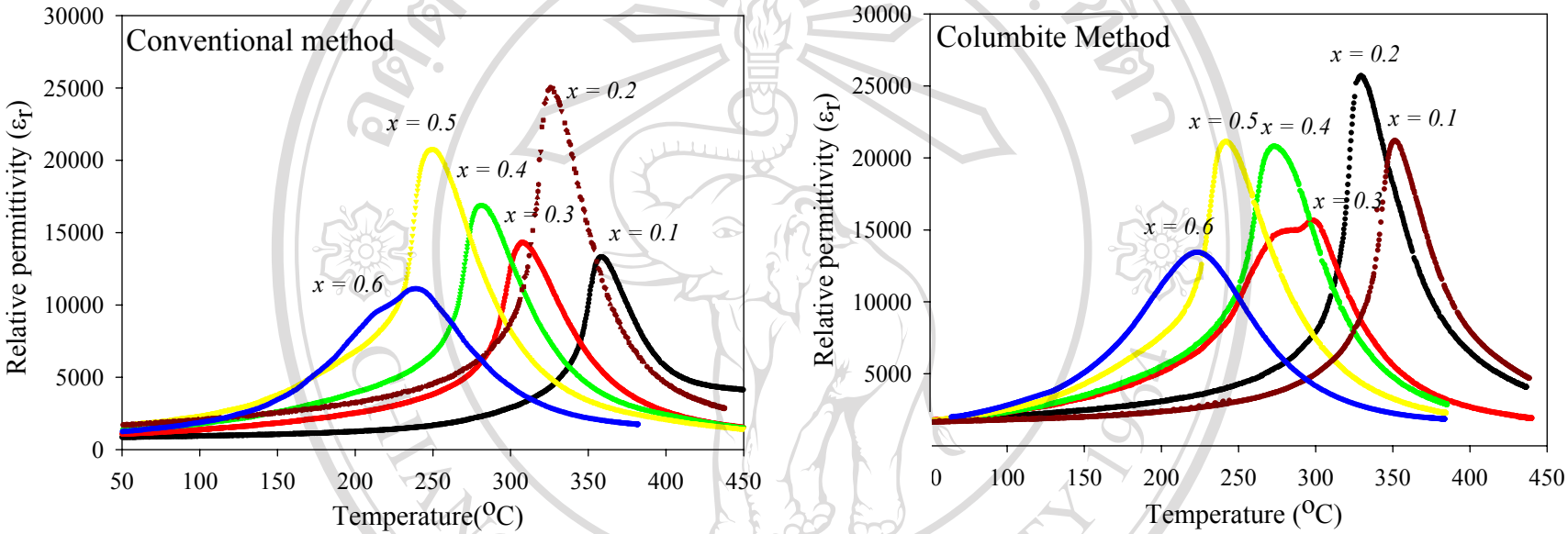

Figure 5.4 Relative permittivity versus temperature curves for the *x*PZN–(*1*-*x*)PZT ceramics.The frequency used for the measurement is 1 kHz: (a) conventional method; and (b) columbite method.

Fig. 5.5 also shows that an increase in PZN mole fraction leads to a decrease in T_{max}. The variation in transition temperature with composition is detailed in Fig. 5.6. The ceramics produced by the columbite method show a slightly lower transition temperature compared to ceramics produced by the conventional method.

A quasi-linear relationship between T_{max} and x is evident. This relationship follows closely to the rule of mixtures, as expressed by:

$$T_{\max} = x(140^{o}C) + (1-x)(390^{o}C) \tag{5.1}$$

where 140°C and 390°C are the T_{max} values for the two constituent compounds PZN and PZT, respectively. From Fig. 5.6, the calculated T_{max} from Eq. (5.2) is slightly higher than the actual transition temperature. Above T_{max}, the ε_r versus T curve for a normal ferroelectric can be described by the Curie-Weiss law. When a normal ferroelectric forms a solid solution with a relaxor, the ε_r versus T relationship follows a similar function with additional variables γ and δ_{γ}:[8,56]

$$\frac{\varepsilon'_m}{\varepsilon'(f,T)} = 1 + \frac{(T - T_m(f))^{\gamma}}{2\delta_{\gamma}^2} \tag{5.2}$$

where ε'_m is the maximum value of the permittivity at $T = T_m(f)$. The value of γ is the expression of the degree of dielectric relaxation in the relaxor ferroelectric material. When γ = 1 Eq. (5.2) expresses Curie-Weiss behavior, while for γ = 2 this equation is identical to the quadratic relationship.[8]

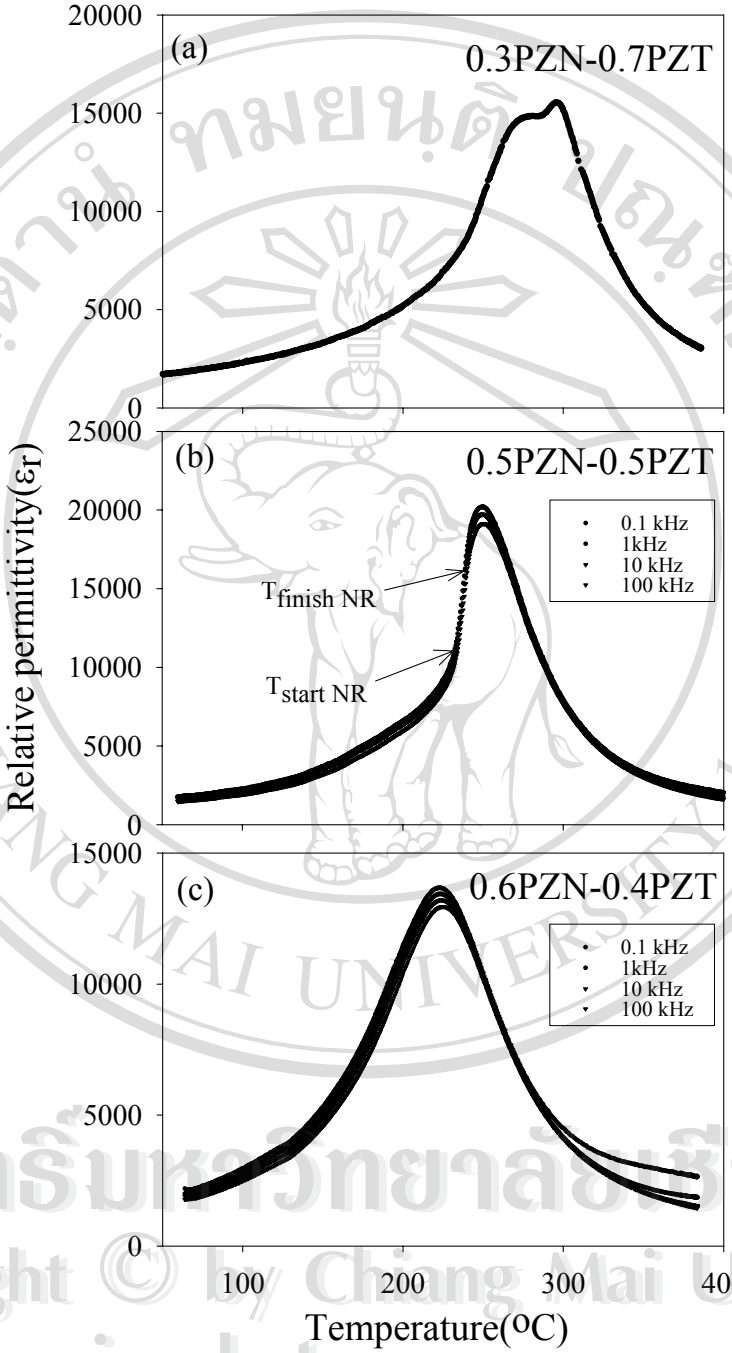

Figure 5.5 Phase transitions detected from the ε_r versus T curves in ceramics prepared via the columbite method, (a) *0.3*PZN–*0.7*PZT ceramic at 1 kHz; and (b) *0.5*PZN–*0.5*PZT ceramic at 0.1, 1, 10 and 100 kHz, and (c) *0.6*PZN– *0.4*PZT ceramic at 0.1, 1, 10 and 100 kHz.

Many relaxor ferroelectric materials can be fit to Eq. (5.2) with $\gamma = 2$ at temperatures above $T_{max.}$ The parameter δ_γ can be used to measure the degree of diffuseness of the phase transition in mixed relaxor-normal ferroelectric materials.[8] Plots of $\log[(\varepsilon_m/\varepsilon)-1]$ vs. $\log(T-T_m)$ for $x = 0.1$ and 0.5 are shown in Fig. 5.7 where linear relationships can be clearly seen. The parameter γ is determined from a slope of the plots to be 1.34 and 1.71 and the diffusiveness parameter δ_γ is the intercept values of 10.7 and 16.7 in ceramics prepared with the columbite method for $x = 0.1$ and 0.5, respectively. As the PZN mole fraction increases, the solid solution displays more relaxor-like characteristics.

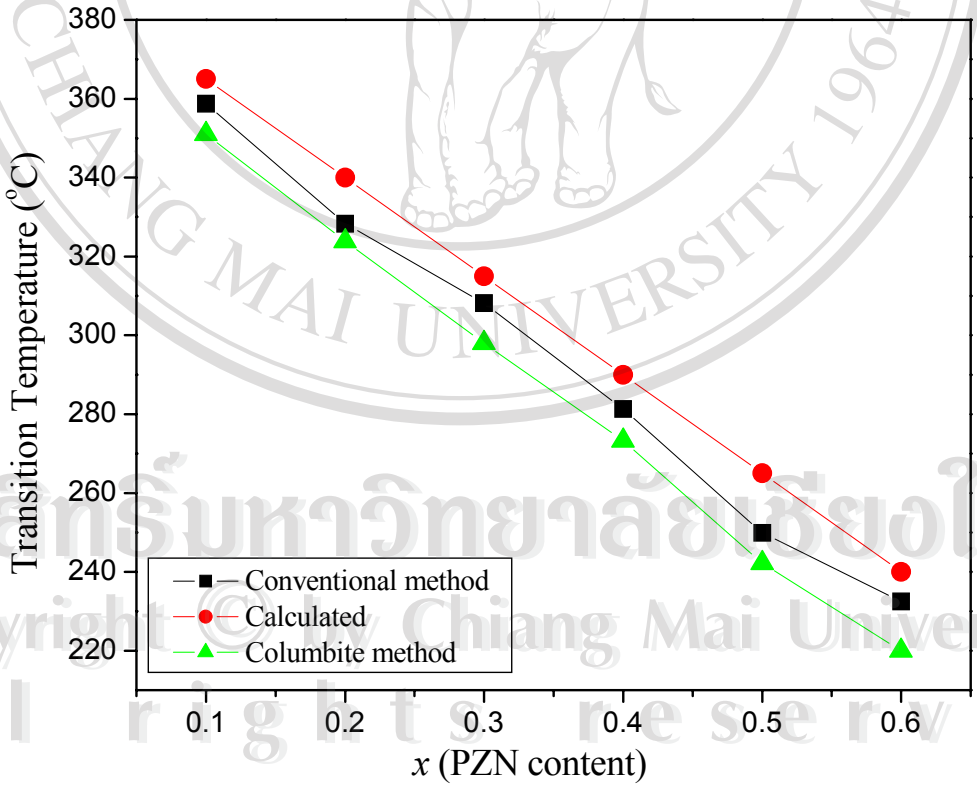

Figure 5.6 Variation of T_{max} with increasing PZN content x in the xPZN–$(1-x)$PZT system.

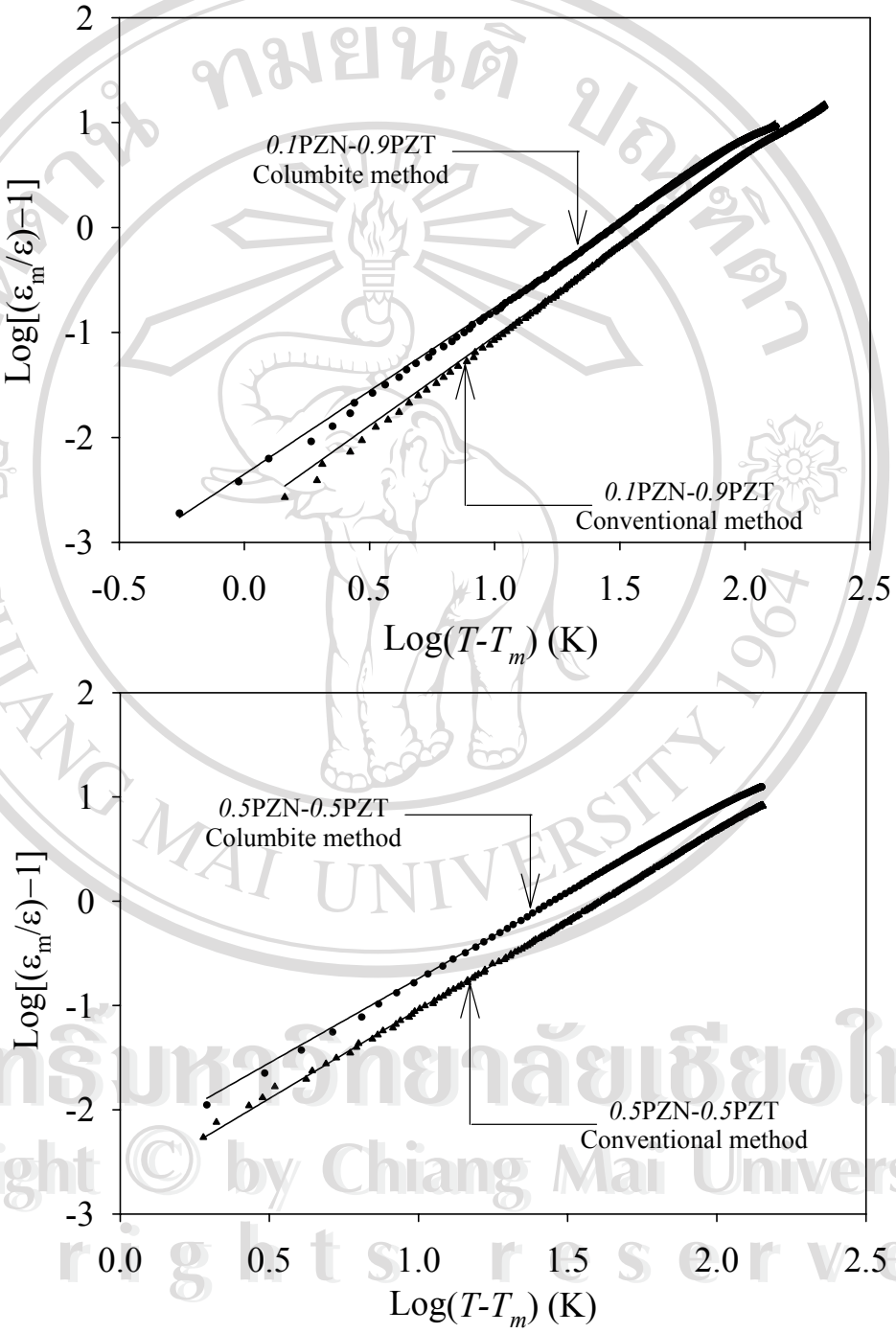

Figure 5.7 The $\log\left[\left(\frac{\varepsilon_{r\max}}{\varepsilon}\right)-1\right]$ vs. $\log(T-T_{\max})$ plots for (a) *0.1*PZN–*0.9*PZT and (b) *0.5*PZN–*0.5*PZT.

5.3.3 The morphotropic phase boundary

On the basis of XRD and ferroelectric hysteresis measurements, the MPB in the xPb($Zn_{1/3}Nb_{2/3}$)O_3–$(1-x)$Pb($Zr_{0.5}Ti_{0.5}$)O_3 system was identified in chapter 4. The MPB sits between $x = 0.2$ and $x = 0.3$, separating the tetragonal phase for $x \leq 0.2$ from the rhombohedral phase for $x \geq 0.3$. This MPB is also confirmed by the dielectric data shown in Fig. 5.4, where the maximum permittivity ε_{rmax} shows a peak at $x = 0.2$. Fig. 5.8 is a replot of the ε_{rmax} *vs.* x in xPZN–$(1-x)$PZT system, presented in Fig 4.9(b)

In addition to the MPB that separates the tetragonal from the rhombohedral phase, there is another transition from normal ferroelectric to relaxor ferroelectric for the rhombohedral phase. Compared to the tetragonal-to-rhombohedral structural transition, this ferroelectric transition is more gradual. However, for the composition of $x = 0.6$ characteristic relaxor ferroelectric behavior is evident, as indicated by the profound dispersion in the dielectric response (Fig. 5.5(c)). Although this ferroelectric transition is not reflected in the E_C measurements, the relative permittivity clearly shows a maximum value in this composition range. In Fig. 5.8, the transition is indicated by a broad shaded line.

The phase transition sequence was also characterized by Raman spectroscopy. Fig. 5.9 shows the Raman spectra for all compositions in this study. There were minor differences between the Raman spectra obtained from samples prepared via the conventional method (Fig. 5.9(a)) and the columbite method (Fig. 5.9(b)). Several features in Fig. 5.9 indicate the phase transition occurs at $x = 0.2 \sim 0.3$. First, there is a shifting of peak locations in the wavenumber range 150-350 cm^{-1}. The change from two definite peaks to the presence of three or more peaks in this range occurs between

x = 0.2 and *0.3*, supporting XRD and ferroelectric hysteresis data. In addition, there are similar changes in the peak profile in the range 475-525 cm^{-1} and 700-800 cm^{-1}. Overall, the Raman data from the columbite prepared samples shows a more distinct change in phase between *x = 0.2* and *0.3*.

Although this ferroelectric transition is not reflected in the E_C measurements, the relative permittivity clearly shows a maximum value in this composition range. In Fig. 5.8, the transition is indicated by a broad shaded line. TEM examination provided supportive evidence for this phase transition sequence in the *x*PZN–*(1-x)*PZT system.

As shown in Fig. 5.10 and 5.11, regular lamellar 90° domain configurations dominate in the tetragonal 0.1PZN–0.9PZT ceramic, while disrupted domains dominate in the rhombohedral 0.5PZN–0.5PZT ceramic with profound relaxor

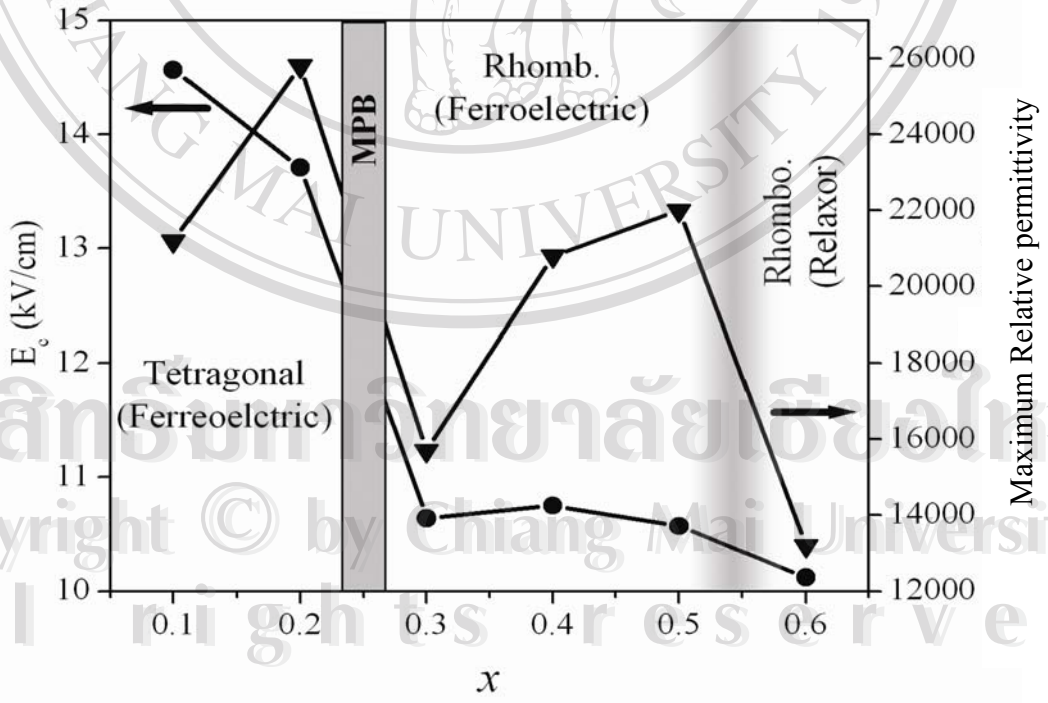

Figure 5.8 Coercive field (E_c) and relative permittivity versus *x* in *x*PZN–(*1-x*)PZT ceramics showing the presence of MPB at *x* ≈ *0.25*

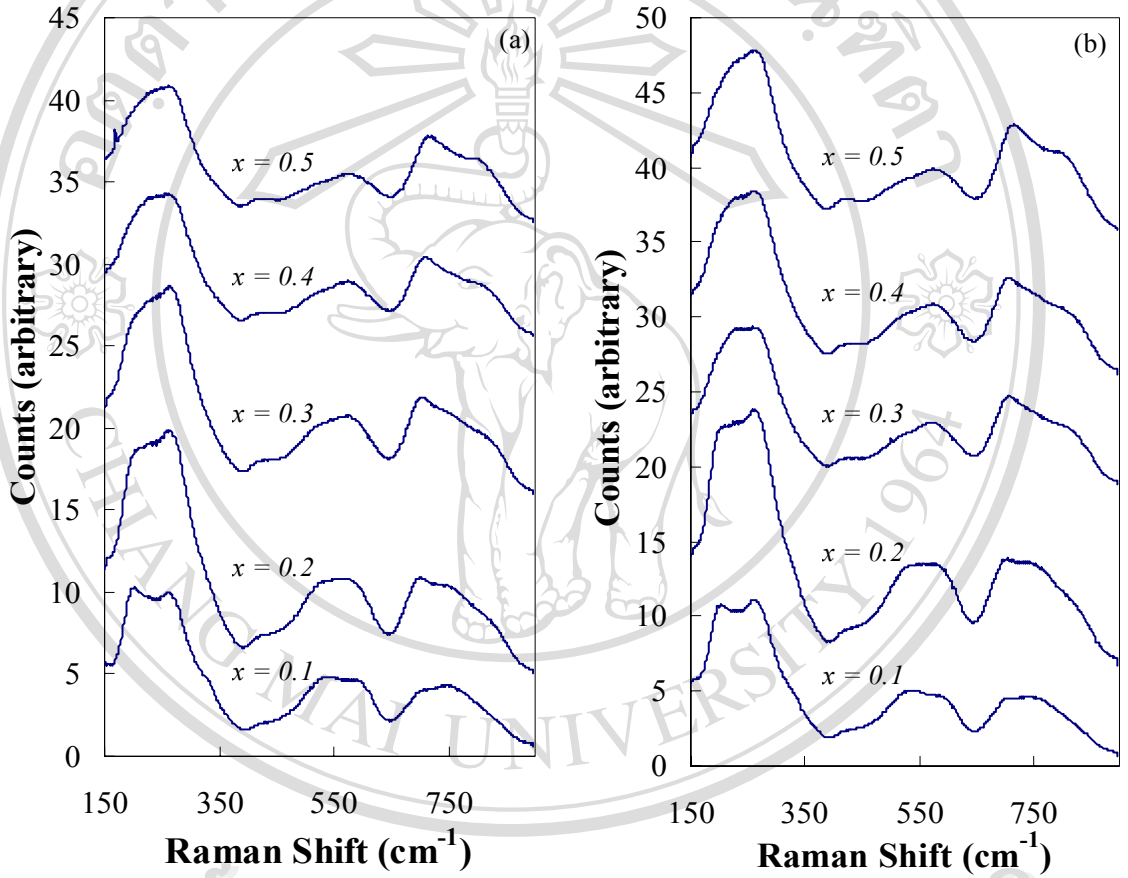

Figure 5.9 Raman spectroscopy curves for *x*PZN–(*1*-*x*)PZT ceramics prepared by (a) conventional and (b) columbite method.

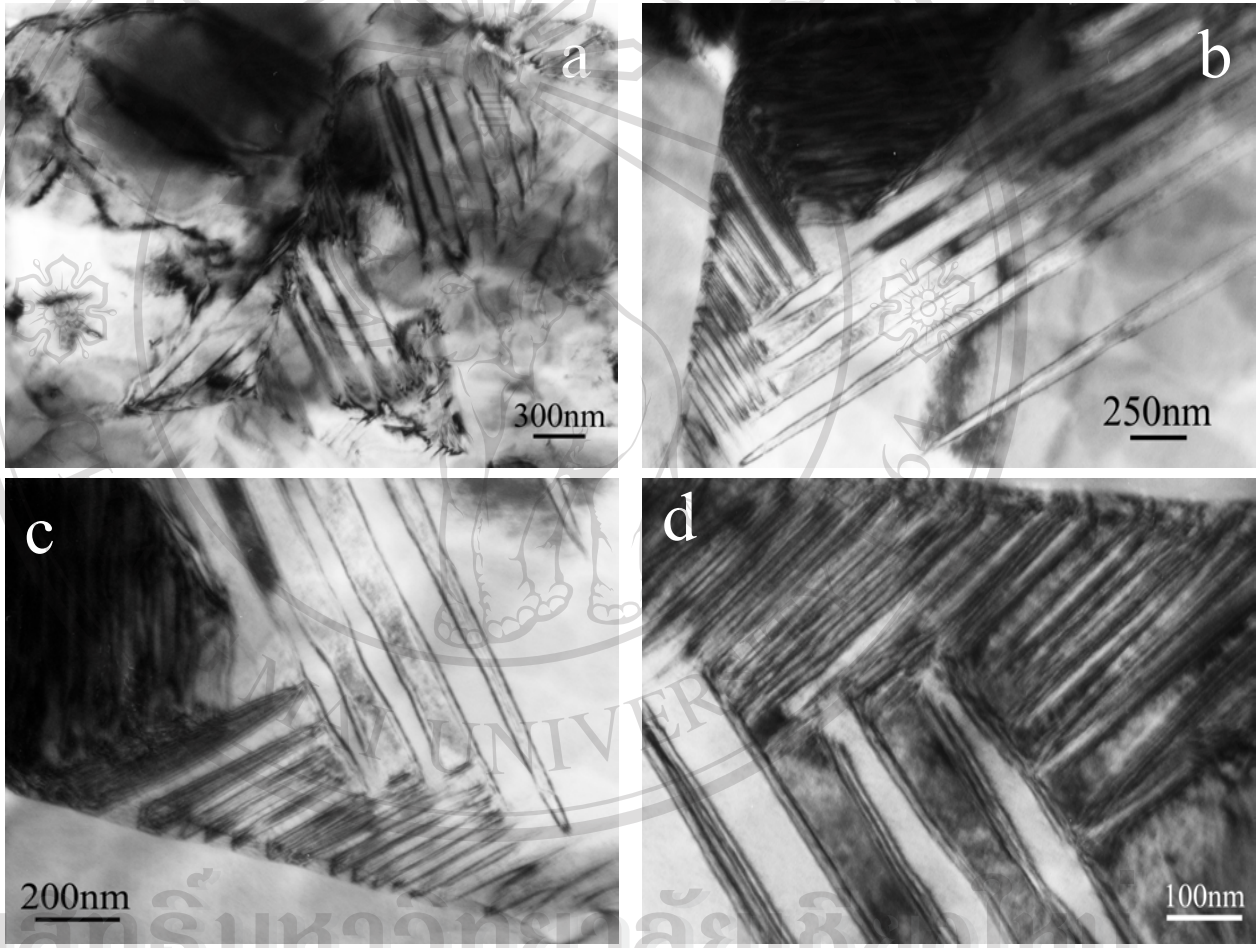

Figure 5.10 TEM micrographs of the *0.1* PZN-*0.9*PZT ceramic;(a-d) shows the evolution of the tetragonal domains.

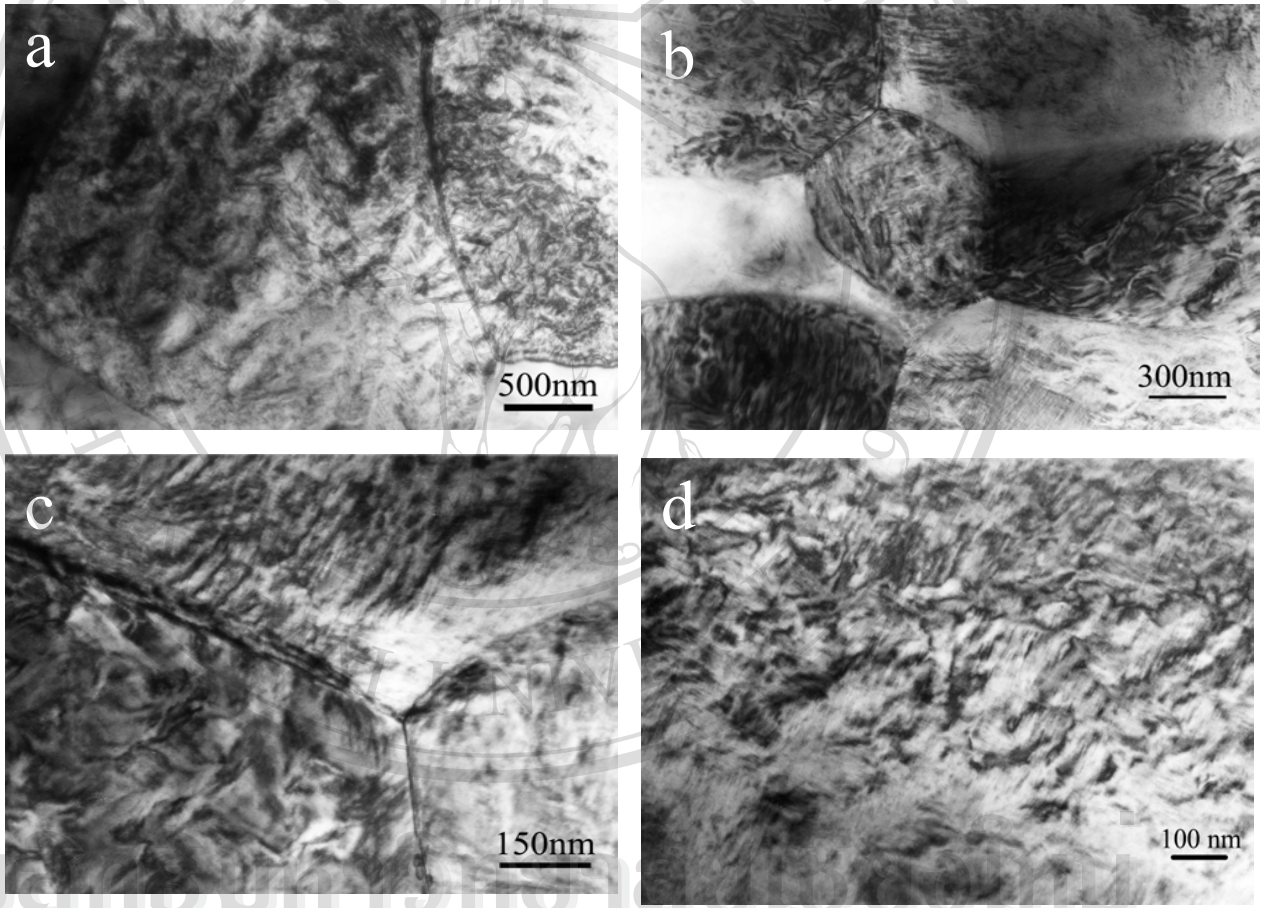

Figure 5.11 TEM micrographs of the *0.5* PZN-*0.5*PZT ceramic; (a-d) shows the evolution of the rhombohedral domain.

5.3.4 Piezoelectric properties

The effect of sintering temperature on the piezoelectric coefficient d_{33} of PZN-PZT ceramics prepared via columbite method is illustrated in Fig. 5.12. The coefficient d_{33} increases with increasing sintering temperature up to 1225°C and then decreases for all compositions. It is clearly apparent that the optimum processing condition is sintering at 1225°C for 2 hours. The lower d_{33} values in ceramics sintered at 1250°C are presumably due to the PbO loss during the sintering process. Also evident in Fig. 5.12 is that the composition *0.3*PZN–*0.7*PZT exhibits the highest piezoelectric coefficient d_{33} among all the compositions. It is interesting to note from Fig. 5.8 that this composition possesses a rhombohedral symmetry at room temperature and is very close to the MPB. The observation is consistent with other relaxor-normal ferroelectric solid solution systems, such as the $Pb(Mg_{1/3}Nb_{2/3})$–$PbTiO_3$ and the $Pb(Zn_{1/3}Nb_{2/3})$–$PbTiO_3$ systems, where ultrahigh piezoelectric properties were found in the rhombohedral phase close to the MPB.[7]

The piezoelectric coefficient d_{33} of the ceramics synthesized via the columbite method sintered at optimum conditions is replotted against the composition parameter x in Fig. 5.13, together with the electromechanical coupling factor k_p. High coupling factor values are noted in compositions of $x = 0.3, 0.4$ and 0.5, among which the composition *0.3*PZN–*0.7*PZT displays the highest values. In Table 5.2, the piezoelectric properties observed in this study are compared with previous reports where the conventional mixed-oxide method was utilized. The enhancement of permittivity and the P_r in ceramics prepared by columbite method is probably due to an increase of domain wall polarizability.

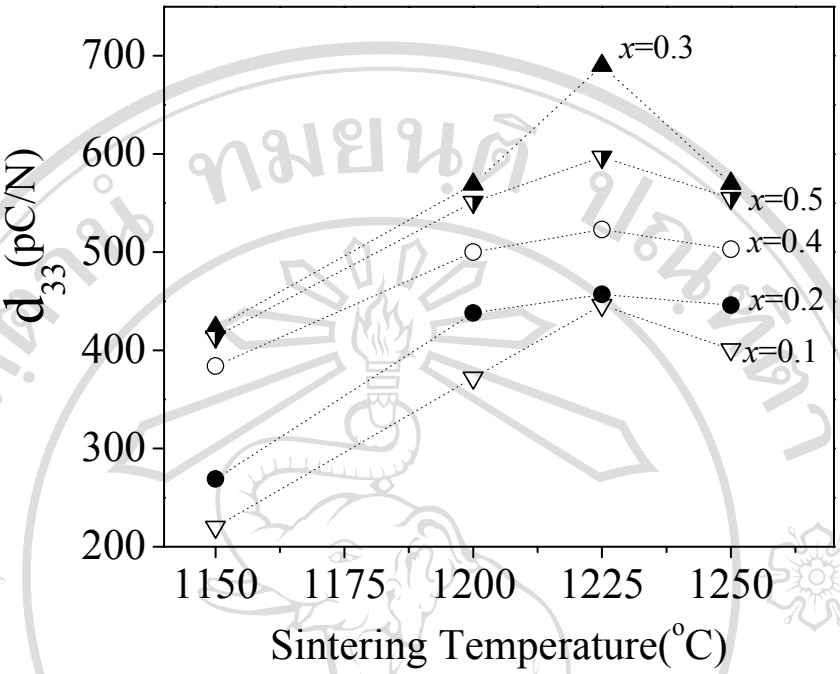

Figure 5.12 Piezoelectric coefficient d_{33} as a function of sintering temperature for xPZN – (1-x)PZT ceramics prepared via columbite method.

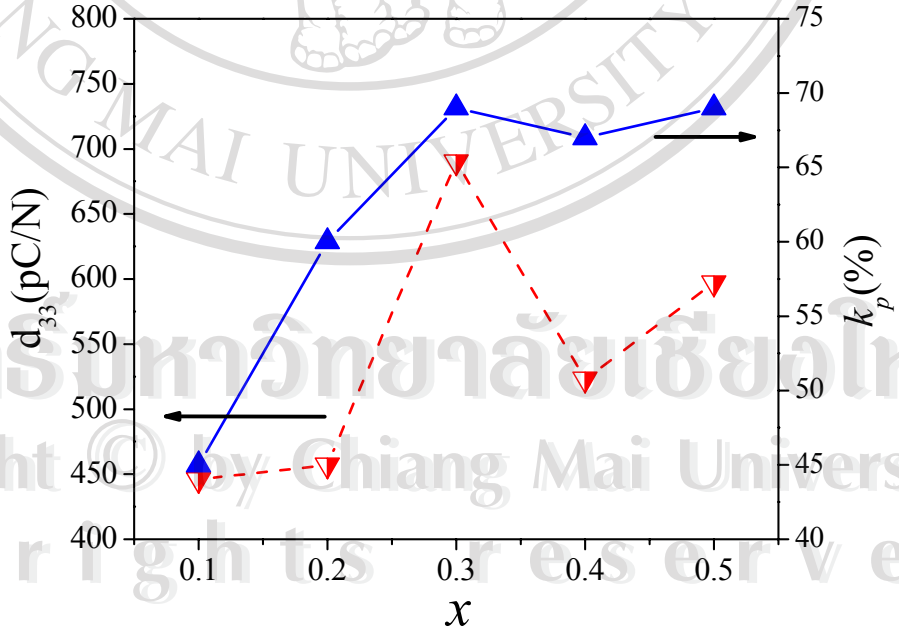

Figure 5.13 Piezoelectric properties d_{33} and k_p in ceramics prepared with optimized processing conditions.

It is clear that the columbite method used in the present study produced ceramics with much better piezoelectric properties.

Table 5.2 Comparison of the piezoelectric properties observed in this study with previous studies.

Materials	Feature	k_p(%)	d_{33}	Reference
PZT53/47	Polycrystalline	52	220	[2]
PZN-PT (91/9)	Single crystal	92	1500	[25]
PST:PT (55/45)	Polycrystalline	61	655	[57]
PMN:PT (67/33)	Polycrystalline	50	235	[58]
PSN:PT (58/42)	Polycrystalline	71	450	[59]
PMN:PT (67/33)	Single crystal		1500	[54]
PZN:PZT(50/50) conventional	Polycrystalline	67	430	[24]
PZN:PZT(30/70) columbite	Polycrystalline	70	690	This study
PZN:PZT(50/50) columbite	Polycrystalline	67	600	This study

5.3.5 The PZN–PZT phase diagram

All the above results can be combined into a phase diagram which shows the complete picture of the ferroelectric $Pb(Zn_{1/3}Nb_{2/3})O_3$–$Pb(Zr_{0.5}Ti_{0.5})O_3$ system (Fig. 5.14). The data used in this phase diagram were derived from the dielectric measurements on columbite-method prepared ceramics. The two data points at x = 0.3 were obtained from the two peaks on the ε_r versus T curve from Fig. 5.5(a). According to this phase diagram, the $0.3Pb(Zn_{1/3}Nb_{2/3})O_3$–$0.7Pb(Zr_{0.5}Ti_{0.5})O_3$ ceramic

transforms from ferroelectric rhombohedral phase to ferroelectric tetragonal phase at 283.6°C and to a paraelectric cubic phase at 298.8°C. The shaded range between $x = 0.5$ and 0.6 denotes a transition from a normal ferroelectric to a relaxor ferroelectric. The best piezoelectric properties were observed in the $0.3Pb(Zn_{1/3}Nb_{2/3})O_3$–$0.7Pb(Zr_{0.5}Ti_{0.5})O_3$ ceramic.

5.4 Conclusions

Investigations on the structure and properties of the $xPb(Zn_{1/3}Nb_{2/3})O_3$–$(1-x)Pb(Zr_{0.5}Ti_{0.5})O_3$ system over the range $x = 0.1 – 0.6$ have revealed a well-defined MPB around $x = 0.25$, separating a tetragonal phase from a rhombohedral phase. A normal ferroelectric to relaxor ferroelectric transition is also observed around $x = 0.5$ to 0.6. This transition corresponds to a gradual decrease in the rhombohedral distortion in the structure and a gradual increase in the frequency dispersion of the dielectric response. Obviously the $0.3Pb(Zn_{1/3}Nb_{2/3})O_3$–$0.7Pb(Zr_{0.5}Ti_{0.5})O_3$ composition has excellent piezoelectric properties.

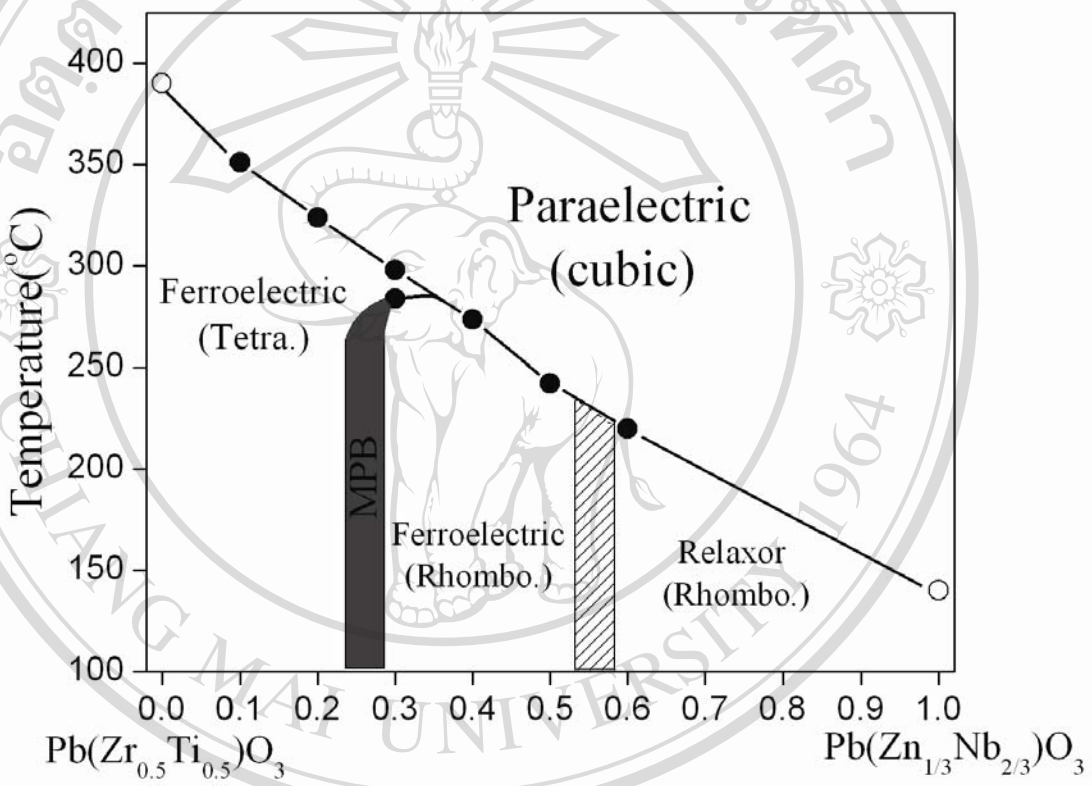

Figure 5.14 The proposed phase diagram for the $Pb(Zn_{1/3}Nb_{2/3})O_3$–$Pb(Zr_{0.5}Ti_{0.5})O_3$ pseudo-binary solid solution system. The solid circles represent data points obtained from the present study, the open circles represent data taken from reference 21.